Accuracy improvement of the transient heater foil technique for heat transfer tests: preliminary results

Julian Schmid[1,3*], *Michele* Gaffuri[1], *Alexandros* Terzis[2], *Peter* Ott[1], and *Jens* von Wolfersdorf[3]

[1] EPFL, Group of Thermal Turbomachinery (GTT), 1015 Lausanne, Switzerland
[2] Stanford University, Department of Mechanical Engineering, CA-94605, USA
[3] University of Stuttgart, Institute of Aerospace Thermodynamics, 70569 Stuttgart, Germany

Abstract. Experimental heat transfer measurements are used in a wide range of fields, for example to validate new cooling concepts in turbomachinery, to assess the performances of heat exchangers, and to provide data for numerical simulations. A particular challenge is posed by complex geometries, where the heat transfer coefficients cannot be determined with the usual transient heater mesh method. One way to address these complex systems is the transient heater foil method, which generates a constant heat flux in the metal foil, which is attached at the surface to be measured. However, the accuracy of the measurement remains an open issue compared to the heater mesh method. Here we show a modification of the heater foil method, which uses a linearly increasing heat flux in the foil to improve the measurement accuracy, especially in low heat transfer regions. The new method is presented using a single impingement cooling setup; results demonstrate good agreement with the baseline method (heater foil with step heating) and the literature, while the accuracy is improved.

Nomenclature

DC	direct current
Nu	Nusselt number [-]
PMMA	Poly(methyl methacrylate)
Pr	Prandtl number [-]
Re	Reynolds number [-]
A	target plate surface area [m^2]
C	discharge coefficient [-]
D	jet diameter [m]
h	heat transfer coefficient [$W/(m^2K)$]
I	current [A]
k	thermal conductivity [$W/(mK)$]
L	orifice thickness [-]
L/D	length-to-diameter ratio [-]
O.D.	outer diameter [mm]
P	power [W]
q	heat flux [W/m^2]
q_0	ramp slope [W/(m^{2}s)]
Q	power [W]
r/D	normalized radial distance [-]
t	time [s]
t_{iR}	indication time (ramp method) [s]
t_{iS}	indication time (step method) [s]
T	temperature [K]
T_0	initial/ambient temperature [K]
T_{aw}	adiabatic wall temperature [K]
T_{DT}	driving temperature [K]
T_{LC}	liquid crystal indication temperature [K]
U	voltage [V]
z	depth coordinate [mm]
Z/D	jet to plate distance [-]
α	thermal diffusivity [m^2/s]
α_T	temperature coefficient [K^{-1}]
Δp	pressure drop [bar]
Δh	relative uncertainty of h [%]
μ	dynamic viscosity [kg/(ms)]
ρ	density [kg/m^3]

1 Introduction

The thermochromic liquid crystal technique is widely used for the determination of the heat transfer coefficient of a flow cooling or heating a solid, for example for the flow through a heat exchanger [1] or the internal [2] and external [3] cooling of a turbine blade. Many variants of this technique exist, which can be divided into steady state and transient. For the steady state technique, heat is applied by a heater foil at the surface and the steady-state temperature, determined by the color of the liquid crystals applied on the surface under consideration, is used to determine the heat transfer coefficient via an energy balance. In the transient case, the needed information is the time required for the surface of the solid to reach a certain temperature, and the heat transfer coefficient can be determined by using the heat equation with suitable boundary conditions. Heat is added to the system either by heating the flow (heater mesh technique) or by applying a heat flux via Joule heating with a thin conductive foil applied to the surface (heater foil technique). The latter is widely used in the frame of film cooling to determine the film cooling

* Corresponding author: julschmid@ethz.ch

effectiveness [4], but has seen applications also for the determination of the heat transfer coefficient [5].

For the transient heater mesh technique, a step in the flow temperature is generated at the beginning of the experiment, and the flow temperature remains constant afterwards. In the case of complex geometries, where the flow can take different paths, this method is not well suited, because the temperature evolution will not be a perfect step, and different flows will be at different temperatures, making it difficult to establish the reference flow temperature at each point. In this scenario, for example in sequential impingement arrays with bypasses between channels [6], heating the surface directly can be an advantage: the upstream flow remains at ambient temperature, so that the fact that several flows mix is not a problem.

A step heater foil technique has been developed to address these complex configurations [6]. Its accuracy, however, is not satisfactory for cases where the surface under consideration experiences very different heat transfer coefficients at different locations, for example in jet impingement cases: when the applied heat flux is constant, the temperature evolution will reach an asymptotic value which depends on the heat transfer coefficient, with higher heat transfer coefficients leading to lower temperatures. Thus, the applied heat flux must be high enough to reach the liquid crystal indication temperature in the high heat transfer regions. However, in this case the low heat transfer regions will have a very short experimental time, leading to a reduced accuracy of the results.

To overcome this issue, the heater foil technique is modified to have a linearly varying heat flux at the surface. The asymptotic temperature evolution is avoided, and the temperature has more of a linear evolution. The slope of the heat flux ramp can thus be freely chosen. In this paper, the technique is outlined and results on a single jet impingement test case are presented, as well as a comparison with data from the literature.

2 Experimental setup and instrumentation

2.1 Experimental setup

Figure 1 shows a schematic representation of the single impingement test facility. The open circuit low speed wind tunnel consists of a dual counter-rotating axial fan which is operated in blowing mode, a settling chamber with honeycombs, a convergent bell mouth and a straight square tunnel (100x100mm^2). At the end of the tunnel (800mm) a chamfered orifice plate is mounted where an impingement hole (D=15mm) is drilled resulting in a nozzle of equal length-to-diameter rate (L/D=1). On both sides, the chamfer of the hole has an angle of 30° and is 1mm deep. The target plate is mounted on four threaded rods to adjust variable distances (Z/D) between the orifice plate and the target plate.

2.2 Instrumentation

Type K thermocouples are mounted upstream of the orifice plate inside the tunnel to evaluate the jet temperature. The ambient temperature was determined close to the target plate, ensuring no influence of the jet. All used thermocouples were calibrated together in a temperature controlled liquid bath (Lauda E4S) using a precision resistance thermometer (Omega DP251) resulting in a maximum deviation of 0.1K.

The flow conditions at the orifice plate were determined using several static pressure tappings to acquire the overall pressure drop across the plate. The used pressure scanner (DSA3217 Scanivalve) offers an accuracy of 0.12% over the full measurement range (1psi). Figure 2 shows the normalized axial velocity profiles traversed with a pitot tube (O.D. 1.9mm) in front of the orifice. For the individual Reynolds numbers, an almost tophat shape distribution was found. The discharge coefficient obtained from the measurements results in an average value of C=0.87. Therefore, during the heat transfer tests, the Reynolds number based on the jet diameter (D) can be obtained as follows:

$$Re = CD\frac{\sqrt{2\rho\Delta p}}{\mu} \quad (1)$$

where C is the discharge coefficient found previously, and Δp the measured pressure drop across the plate. The uncertainty in the determination of the Reynolds number was always below 4%, similar to previous experiments carried out on this setup [7].

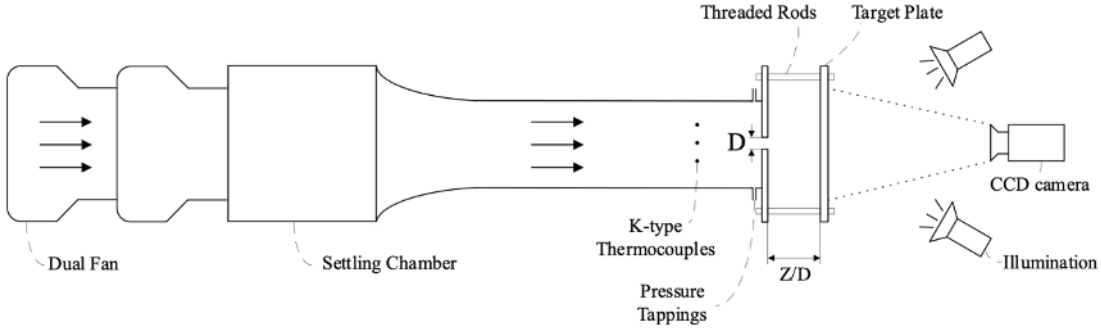

Fig 1. Schematic representation of the experimental setup

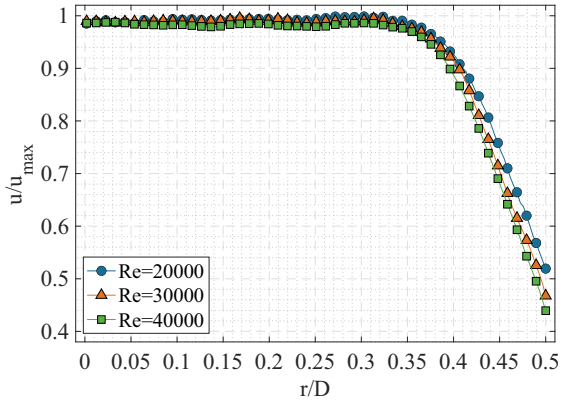

Fig. 2. Velocity profiles for different Reynolds numbers

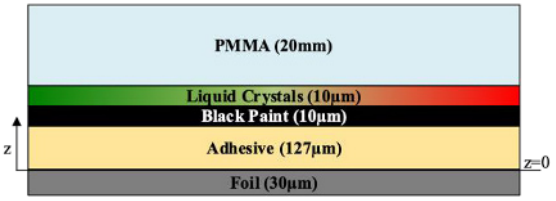

Fig. 3. Schematic representation of the target plate, layer thicknesses not to scale.

The electrical power required to use the heater foil as a surface energy source is provided by a DC power supply in voltage control mode, capable of reaching a maximum voltage and current of 40V and 128A. The voltage drop across the foil was measured at the attached copper bars. A shunt resistor (CEWE 100A 60mV ±0.5%) is used to ensure accurate measurement of the current. From the resulting voltage drop across the resistor, the current can be calculated. The power generated by the foil can be obtained using the relation P=UI, which depends on the electrical resistance of the foil. All measurement signals were acquired with TI DAQs.

The color evolution of the liquid crystals was recorded with a CCD camera (AVT Pike F-210C) at a frame rate of 15Hz in lossless quality, the spatial resolution of the observed area varied between 4.25-4.9pixel/mm depending on the distance of the target plate (Z/D).

2.3 Test model

A schematic representation of the target plate is shown in Figure 3. A transparent PMMA plate (20mm) is painted with thermochromic liquid crystals (Hallcrest R38C1W) and black paint (Hallcrest SPB 100). The thickness of the paint layers was found to be 10±1µm. A 30µm thick metal foil made of Kanthal D (1.4767), which has a low temperature coefficient (α_T=0.0193 K^{-1}), is bonded to the black paint with a highly thermally conductive adhesive tape (0.127mm). At the lateral ends, the foil is clamped between copper bars, which distribute the electrical power evenly over the foil. The available area for heat transfer coefficient evaluation is equal to a radial distance of r/D=5 where r/D=0 is the geometrical stagnation point.

3 Methods

3.1 Transient measurement technique – Step heater foil

The transient liquid crystal technique previously applied for impingement studies at GTT used mainly the heater mesh technique [7,8]. A variation in form of using the heater foil was developed and applied in various contexts [4,6,9]. At time t=0, instead of causing a step change in fluid temperature an electric current is passed through the heater foil, which generates a power Q that provides a constant local heat flux q=Q/A, where A is the foil area. Ideally, the model and the flow are initially at ambient temperature; however, this is not possible in blowing mode as the fan raises the jet temperature by about 5-10K depending on the flow condition. An entrainment effect correlation is applied to correct the influence of the increased jet temperature [10] at the start of the experiment t=0. Therewith the local adiabatic wall temperature T_{aw} is related to measurements of the jet and ambient temperatures. In order to keep the model at ambient temperature, the jet is redirected and hits the target plate first at time t=0.

During the experiment, the temperature evolution of the target plate can be monitored by observing the color change of the liquid crystals, since the relation between color and temperature was previously determined by calibration. For the determination of the heat transfer coefficient from the recorded data, the one-dimensional heat conduction equation (2) can be solved by assuming the solid to be semi-infinite:

$$\frac{\partial^2 T(z,t)}{\partial z^2} = \frac{1}{\alpha}\frac{\partial T(z,t)}{\partial t} \tag{2}$$

with the initial condition:

$$T(z, t=0) = T_0 \tag{3}$$

and the boundary conditions:

$$T(z \to \infty, t) = T_0 \tag{4}$$

$$-k\frac{\partial T(0, t>0)}{\partial z} - h[T_{aw} - T(0,t)] = q \tag{5}$$

Where α and k are the thermal diffusivity and thermal conductivity of the target plate (PMMA) and T_{aw} the adiabatic wall temperature. Based on the adiabatic wall temperature T_{aw} and the heat flux q generated by the foil, an equivalent driving temperature $T_{DT} = T_{aw} + q/h$ can be defined to simplify the boundary condition and describe the process in terms of temperature differences.

$$-k\frac{\partial T(0, t>0)}{\partial z} - h[T_{DT} - T(0,t)] = 0 \tag{6}$$

The general solution to this problem can be found using [11]:

$$\frac{T(z,t)-T_0}{T_{DT}-T_0} = \operatorname{erfc}\left(\frac{z}{2\sqrt{\alpha t}}\right) - e^{\left(\frac{hz}{k}+\alpha t\frac{h^2}{k^2}\right)}\operatorname{erfc}\left\{\frac{z}{2\sqrt{\alpha t}}+\frac{h}{k}\sqrt{\alpha t}\right\} \quad (7)$$

If the time t required to reach a specific temperature T_{LC} at the liquid crystal layer (z=0.137mm) is known, the heat transfer coefficient h can be calculated pixel-wise numerically using the equation above. Note that this model assumes that the adhesive film and the black color have thermal properties similar to those of the PMMA plate and a uniform temperature within the heater foil in z-direction.

3.2 Transient measurement technique – Ramp heater foil

The new ramp method is based on the idea of ramp heating [12], where instead of a step-change, a linear increase in driving temperature is performed throughout the experiment. Therefore, the generated heat flux of the foil increases linearly with time. The boundary condition changes as follows:

$$-k\frac{\partial T(0,t>0)}{\partial z} - h[T_{aw} - T(0,t)] = q_0 \cdot t \quad (8)$$

where q_0 is the slope of the linearly increasing heat flux in W/(m^2 s). Note that due to the new time dependence of the boundary condition, the equivalent driving temperature term cannot be kept in the solution, and the terms must be separated. The solution of equation (2) with the boundary condition (8) is the following:

$$\begin{aligned} T(z,t) - T_0 &= \\ &= (T_{aw} - T_0)\left[\operatorname{erfc}(a) - e^{\left(\frac{hz}{k}+b^2\right)}\operatorname{erfc}(a+b)\right] \\ &+ \frac{q_0}{k\alpha^2}\left[\frac{\alpha}{\left(\frac{-h}{k}\right)^3}e^{\left(\frac{hz}{k}+b^2\right)}\operatorname{erfc}(a+b) - \frac{\alpha}{\left(\frac{-h}{k}\right)^3}\sum_{r=0}^{2}\left(-2\frac{h}{k}\sqrt{\alpha t}\right)^r i^r\operatorname{erfc}(a)\right] \end{aligned} \quad (9)$$

where $a = \frac{z}{2\sqrt{\alpha t}}$ and $b = \frac{h}{k}\sqrt{\alpha t}$ are introduced to simplify the expression.

In Figure 4, the temperature histories for two different heat transfer coefficients are given, for the step and the ramp method. The asymptotic curve of the step method shows that for low h the indication temperature of the liquid crystals is reached fast, which leads to increased uncertainty (Table 1). If the selected heat flux is too low, the indication temperature T_{LC} is not reached in regions with higher h, and several tests have to be performed to determine the heat transfer coefficients of the entire domain. In contrast, the almost linear temperature evolution of the ramp method leads to lower uncertainties (mainly because $t_{iR} > t_{iS}$), and all the domain can be evaluated in a single test.

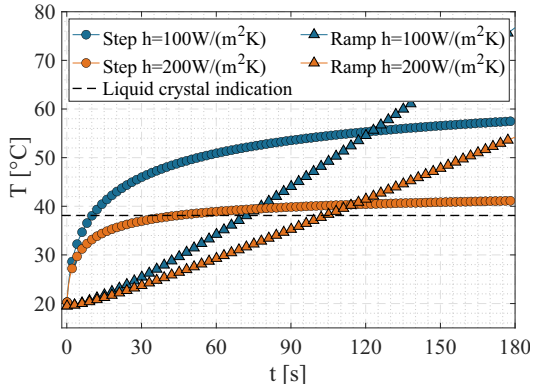

Fig.4. Evolution of temperature for the step (q=5000W/m^2) and ramp (q_0=50W/m^2s)) method at z=0.137mm

3.3 Uncertainty calculation

The experimental uncertainties shown in the results were calculated based on the method of small perturbations, which uses the root sum square technique to combine single uncertainty terms of the measured parameters to estimate the overall uncertainty of the heat transfer coefficient [13].

$$\Delta h = \sqrt{\sum_{i=0}^{n}\left(\frac{\partial h}{\partial x_i}\right)^2 \Delta x_i^2} \quad (10)$$

Assuming that the uncertainty of each parameter is statistically independent and normally distributed, the error can be calculated using equation (10), in which we consider a 2σ (95%) confidence interval. A detailed uncertainty analysis is shown in Table 1.

4 Results and Discussion

4.1 Introductory remarks

The distribution of the measured heat transfer coefficients in the experiments showed an excellent symmetry across the foil. However, to reduce noise the presented results for the local Nusselt distributions are an average value of all pixels located at the same distance (r/D) from the stagnation point.

4.2 Step heater foil method

The suitability of the experimental setup was first tested with the known step method and compared to the correlation of Goldstein and Franchett [14]. The main test case considered a jet to plate distance Z/D=6, and a flow rate leading to Re=30000. For comparability, the results are divided by $Re^{0.7}$, which is assumed due to the well-known power law relation $Nu_D\ Re^m$, where typical m values vary between 0.5 for laminar flow stagnation point regions and 0.8 for turbulent flow wall jet regions.

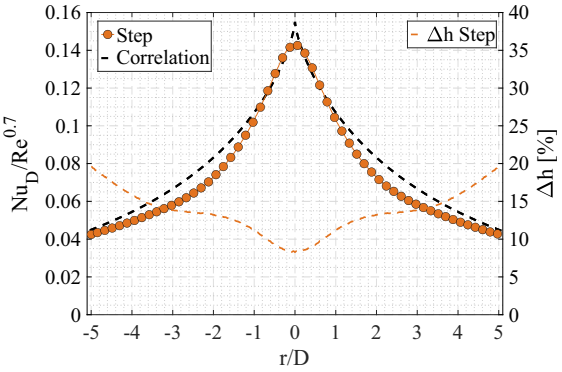

Fig. 5. Local Nusselt number distribution and uncertainty level of the step heater foil method at Re=30000, Z/D=6 with a heat flux of q=3000 W/m^2 in comparison to the correlation [14].

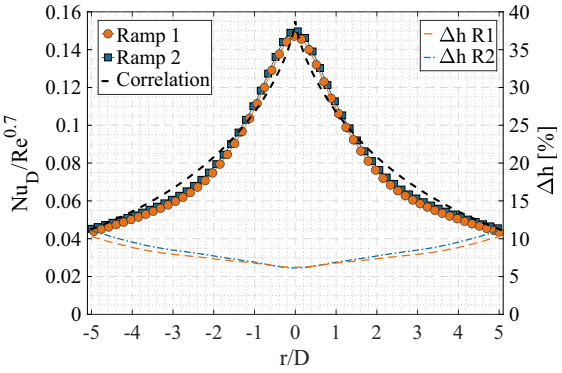

Fig. 6. Local Nusselt number distribution and uncertainty level of the ramp heater foil method at Re=30000, Z/D=6 with varying ramp slopes (ramp 1: q_0=50W/(m^2 s), ramp 2: q_0=75 W/(m^2 s)), in comparison to the correlation [14].

Figure 5 shows the Nusselt number distribution over the normalized radial distance compared to the correlation [14] and the calculated (Eq.10) uncertainty level for this test case. Considering the confidence interval, the step results are within the deviations, which indicates a validation of the setup. The deviations from the correlation are attributed to the different nozzle geometry and test procedure (steady state vs. transient). It should be noted that with the step method, a suitable heat flux must be set; otherwise, the heat transfer coefficient across the entire domain cannot be measured within one experiment due to the asymptotic behavior of the temperature evolution. As a consequence, the indication time t_{iS} in the low heat transfer region is very short relative to the total experimental time, which increases the relative uncertainty level particularly in the wall jet region r/D >3.5. In the stagnation point, which reaches the indication temperature very late, the uncertainty level is lower. In comparison to the heater mesh method, an inverse behavior of uncertainty is observed, since there the highest relative uncertainties occur at the stagnation point.

4.3 Ramp heater foil method

The results of the ramp heater foil method are shown in Figure 6. Contrary to the step method, the ramp slope can be varied and still maintain the results for the heat

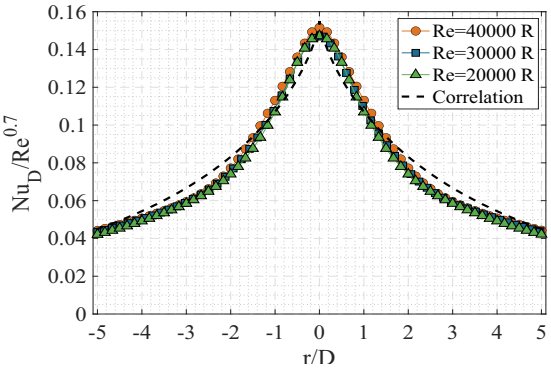

Fig. 7. Local Nusselt distribution of the ramp heater foil method at Z/D=6 and varying Reynolds numbers with a ramp slope of q_0=50W/(m^2 s) in comparison to the correlation [14].

transfer coefficients for the whole domain within one experiment. The only limitation is the compliance with the maximum experiment time, which is given by the semi-infinite assumption. Different ramp slopes provide similar Nusselt number values, but with decreasing gradient q_0 (increasing indication time t_{iR}) a reduction of the relative uncertainty can be found, especially in areas with low heat transfer coefficients.

In general, a flattened course of the uncertainty can be observed compared to the step method, which is mainly due to the linear temperature evolution of the new method. The results are within the confidence interval of the step method and literature data.

In order to show the independence of the new method from the test case, the Reynolds number was varied at a fixed distance Z/D=6 for a ramp gradient q_0=$50W/(m^2s)$ and the distance was varied at a constant Reynolds number Re=30000. The variation of the Reynolds number shows only small deviations from the correlation, and in general, the results are very similar to each other (Figure 7). For the distance variation, it should be noted that only distances Z/D≥6 were considered because below this distance, the influence of the semi-confined setup is visible in the results.

As expected, the heat transfer coefficients decrease with increasing distance (Figure 8). Differences in the experimental setup could cause the deviations from the correlation, especially in the region of r/D>3.

In both variations, results are in agreement with the correlation, thus the independence from the flow conditions and jet to plate distance can be shown for the new ramp method.

4.4 Experimental Uncertainties

Table 1 shows the calculated individual components contributing to the overall uncertainty of the heat transfer coefficient for the step (q=3000 W/m^2) and the ramp (q_0 = $50W/m^2\,s$) methods at Z/D = 6 and Re = 30000. The selected values correspond to locations near the stagnation point (h=$350W/(m^2K)$) and in the wall jet region (h=$120W/(m^2K)$).

For the step method, the relative error at the stagnation point is approximately 8% and increases to 15% in low heat transfer regions, while for the ramp

method the error at the stagnation point is 6% and 9% in

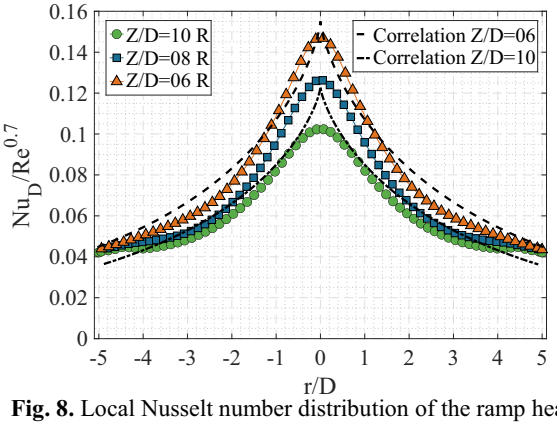

Fig. 8. Local Nusselt number distribution of the ramp heater foil method at Re=30000 and varying jet to plate distances with a ramp slope of q_0=50 W/(m^2 s) in comparison to the correlation [14]

low heat transfer regions. Thus, it can be concluded that the new ramp method improves the relative uncertainty, especially in the low heat transfer regions, due to a more uniform temperature evolution and the later occurrence of the indication temperature of the liquid crystals. The main contributors to the overall uncertainty are the material properties (thermal conductivity, thermal diffusivity), the uncertainty from the used entrainment effect correlation and the accuracy of the measurement of heat flux and ramp gradient.

An analysis of the lateral heat conduction in the foil at the stagnation point showed that the maximum value for the ramp method is 0.3% of the used heat flux, while for the step method it is 0.4%. The low values indicate that lateral heat conduction influences the results only slightly, and can therefore be neglected.

Table 1. Detailed Uncertainties for Re=30000, Z/D=6

	Ramp		Step	
	High h 350 $\frac{W}{m^2K}$	Low h 120 $\frac{W}{m^2K}$	High h 350 $\frac{W}{m^2K}$	Low h 120 $\frac{W}{m^2K}$
T_0	0.06%	0.20%	0.28%	1.18%
T_g	0.10%	0.01%	0.14%	0.01%
T_{LC}	0.30%	0.13%	0.45%	0.26%
q_0	1.15%	1.61%	-	-
q	-	-	1.71%	2.09%
η	3.02%	0.16%	4.09%	0.18%
α	0.42%	1.63%	0.44%	2.69%
k	1.00%	5.04%	1.11%	8.16%
z	0.08%	0.09%	0.07%	0.17%
t_{LC}	0.01%	0.01%	0.01%	0.01%
Δh	6.14%	8.88%	8.30%	14.75%

5 Conclusion

This study presented preliminary results of a modified heater foil method obtained on a single impingement setup. By using a linearly varying heat flux in the foil instead of a step change, it is possible to avoid the asymptotic temperature behavior of the step method, which allows for an improvement of the measurement accuracy. It also provides the ability to test cases with a wide range of heat transfer coefficients within one experiment, which is only possible with the step method with a loss of accuracy in low heat transfer regions. The variation of the ramp slope showed that the results are independent of the chosen slope, but the accuracy can be improved by using slower ramps, especially in the low heat transfer regions. A comparison with the data from the literature showed that the ramp method is suitable and can be used under different flow conditions and jet to plate distances. The detailed uncertainty analysis showed that the material properties and the measurement of the heat flux significantly influence the accuracy.

The authors would like to acknowledge the Swiss Federal Office of Energy and Ansaldo Energia Switzerland for the funding of this research.

References

1. M. Fiebig, A. Valencia, and N. K. Mitra, “Wing-type vortex generators for fin-and-tube heat exchangers,” *Exp. Therm. Fluid Sci.*, **7**, 4, pp. 287–295 (1993)
2. R. Poser and J. von Wolfersdorf, “Liquid Crystal Thermography for Transient Heat Transfer Measurements in Complex Internal Cooling Systems,” *Heat Transf. Res.*, **42**, pp. 1–13 (2009)
3. F. Satta and G. Tanda, “Measurement of local heat transfer coefficient on the endwall of a turbine blade cascade by liquid crystal thermography,” *Exp. Therm. fluid Sci.*, **58**, pp. 209–215 (2014)
4. G. Vogel, A. B. A. Graf, J. Von Wolfersdorf, and B. Weigand, “A novel transient heater-foil technique for liquid crystal experiments on film-cooled surfaces,” *J. Turbomach.*, **125**, 3, pp. 529–537 (2003)
5. J. Von Wolfersdorf, R. Hoecker, and T. Sattelmayer, “A hybrid transient step-heating heat transfer measurement technique using heater foils and liquid-crystal thermography,” *J. Heat Transf.*, **115**, 2, pp. 319–324 (1993)
6. M. Gaffuri, A. Terzis, and P. Ott, “Evaluation of Heat Transfer Coefficients for an Impingement Cooling Cascade: Experimental Challenges and Preliminary Results,” in *XXIV Biannual Symposium on Measuring Techniques in Turbomachinery* (2018)

7. O. Caggese, G. Gnaegi, G. Hannema, A. Terzis, and P. Ott, "Experimental and numerical investigation of a fully confined impingement round jet," *Int. J. Heat Mass Transf.*, **65**, pp. 873–882 (2013)
8. A. Terzis, P. Ott, J. Von Wolfersdorf, B. Weigand, and M. Cochet, "Detailed heat transfer distributions of narrow impingement channels for cast-in turbine airfoils," *J. Turbomach.*, **136**, 9, (2014)
9. M. Jonsson, D. Charbonnier, P. Ott, and J. von Wolfersdorf, "Application of the Transient Heater Foil Technique for Heat Transfer and Film Cooling Effectiveness Measurements on a Turbine Vane Endwall," Proc. Asme Turbo Expo 2008, **4**, Pts A B, pp. 443–453 (2008)
10. R. J. Goldstein, K. A. Sobolik, and W. S. Seol, "Effect of Entrainment on the Heat Transfer to a Heated Circular Air Jet Impinging on a Flat Surface," *J. Heat Transfer*, **112**, pp. 608–611 (1990)
11. H. S. Carslaw and J. C. Jaeger, *Conduction of Heat in Solids*, 2nd ed., vol. 2. Oxford at the Clarendon press (1959)
12. H. Ma, Z. Wang, L. Wang, Q. Zhang, and Y. Bao, "Ramp Heating in High-Speed Transient Thermal Measurement with Reduced Uncertainty," *J. Propuls. Power*, **32**, 5, pp. 1190–1198 (2016)
13. S. J. Kline, "Describing Uncertainty in Single Sample Experiments," *Mech. Eng.*, **75**, 1, pp. 3–8 (1953)
14. R. J. Goldstein and M. E. Franchett, "Heat transfer from a flat surface to an oblique impinging jet," *J. Heat Transfer*, **110**, 1, pp. 84–90 (1988)